

Effect of seat belt pretensioners on human abdomen and thorax: Biomechanical response and risk of injuries

Costin D. Untaroiu, PhD, Dipan Bose, PhD, Yuan-Chiao Lu, MSc, Patrick Riley, PhD, David Lessley, MSc, and Mark Sochor, MD, Charlottesville, Virginia

-
- BACKGROUND:** A better coupling of the occupant to the car seat in the early phase of a frontal or far side impacts using pretensioner systems may reduce the likelihood of the submarining effect or increases the likelihood of seat belt engaging the shoulder, respectively. However, the high belt forces may also increase the risk of upper body injuries to the vehicle occupant (especially in abdominal region). It was hypothesized that human body characteristics, such as body mass index (BMI) influence the biomechanical response and injury outcome to the abdominal regions during static pretensioning deployment tests.
- METHODS:** Four postmortem human specimens (PMHS), in a BMI range from 15.6 to 31.2, were positioned in production seats in a normal passenger position and were restrained using a standard three-point belt system. The pretension forces in the belts were generated at two points (retractor and right anchorage) or at all three locations (retractor, left anchorage, and right anchorage). An optical motion capture system and acceleration cubes mounted to the lumbar spine were used to measure the abdomen deformation during testing.
- RESULTS:** The normalized deflections of the thorax recorded at the level of fourth rib were under 10% (noninjury level). Two different patterns were observed in the time histories of abdominal penetration rate in the four PMHSs associated with lower and higher BMI. Abdominal injuries (spleen lacerations) were observed only in the two PMHS with highest BMI.
- CONCLUSION:** Based on data from this study and similar data from the literature, belt velocity and $F_{\max}C_{\max}$ were shown to be the best injury predictors for injury risk analysis for Abbreviated Injury Scale 2+ and for Abbreviated Injury Scale 3+ injuries, respectively. (*J Trauma*. 2012;72: 1304–1315. Copyright © 2012 by Lippincott Williams & Wilkins)
- KEY WORDS:** Abdomen; thorax; pretensioning; injury criteria; PMHS testing; injury risk analysis; traffic accidents; vehicle restraint systems.
-

The seat belt is recognized to be the most important safety equipment in a vehicle. It is estimated that three-point seat belts reduce the likelihood of driver fatality and the likelihood of moderate to serious injury by ~45% and 60%, respectively.¹ Current advances in seat belt technology aim to further improve safety performance by optimizing the time histories of belt force during a crash.^{2,3}

A common understanding in occupant protection is that better coupling of the occupant to the car seat in the early phase of a frontal crash avoids head-vehicle contact and reduces the submarining effect.⁴ In addition, a faster coupling of occupant in the car seat increases the likelihood of seat belt engaging the shoulder and consequently the level of restraint provided to occupants in far-side impacts.⁵ To realize this coupling, pyrotechnical devices, called pretensioners, are introduced in the current restraint systems to develop high pull-out forces in a short time period. However, it is known

that high and faster belt forces may produce thoracic and abdominal injuries to vehicle occupants. Therefore, the biomechanical response of the abdomen under belt loading and the incidence of injuries were investigated in several previous studies.

Initial investigations of abdominal response to seat belt loading used animal models. Miller⁶ conducted 25 impacts on anesthetized swine at combinations of velocity and abdominal compression varying from 1.6 m/s to 6.6 m/s and from 6% to 67%, respectively. Maximum compression, maximum viscous response, and peak force-maximum compression were observed to correlate well to abdominal injury risk (Abbreviated Injury Scale [AIS] score 3+).

Hardy et al.⁷ tested three postmortem human specimens (PMHSs) under the lap belt loading (horizontal position) in different configurations: with lap belt positioned initially on mid-abdomen or lower abdomen and with the back free or fixed. The belt velocity ranged between 2 m/s and 5.6 m/s and the abdominal compression between 26% and 36%. No soft tissue injuries were observed; however, rib fractures were observed in two PMHSs.

Steffan et al.⁸ tested 14 PMHSs positioned in a rigid seat under lap belt loading. The belt was fixed at one end to the seat and a cinching device was used to pull the belt to the other end. A step and hold load was applied at a cinching speed of 6 m/s. The peak forces ranged from 3.2 kN to 7 kN and the constant (stabilized) forces between 2 kN and 4.4 kN.

Submitted: July 13, 2011, Revised: September 25, 2011, Accepted: December 16, 2011.
From the Virginia Tech and Wake Forest University School of Biomedical Engineering and Sciences, Virginia Tech, (C.D.U., Y.-C.L.), Blacksburg, Virginia, and the Departments of Mechanical and Aerospace Engineering (D.B., P.R., D.L.) and Emergency Medicine (M.S.), University of Virginia, Charlottesville, Virginia.

Address for reprints: Costin Daniel Untaroiu, PhD, Virginia Tech and Wake Forest University School of Biomedical Engineering and Sciences, Center for Injury Biomechanics, 2280 Kraft Drive, Blacksburg, VA 24060; email: costin@vt.edu.

DOI: 10.1097/TA.0b013e3182472390

TABLE 1. Test Matrix and PMHS Characteristics

Test	PMHS No.	Sex	Height (m)	Mass (kg)	BMI (kg/m ²)	Age (yr)	Abdomen Depth (mm)	Pretensioning Type
1	477	F	1.57	77	31.2	71	285	Triple
2	478	M	1.78	77	24.3	70	238	Double
3	459	M	1.91	57	15.6	64	180	Double
4	458	M	1.80	68	20.9	70	207	Double

Belt penetration rates and abdominal compression ranged from 8.2 m/s to 11.7 m/s and from 25% to 35%, respectively. However, it should be mentioned that the belt penetration and speed were measured not from measured motion at the umbilicus but by using the travel of the lateral aspect of the belt. Injuries (small intestine ruptures) were observed only in three PMHSs with high force peaks (6–6.2 kN).

Trosseille et al.⁹ tested six fixed-back PMHSs and the Thor dummy (version 1998) under dynamic and quasistatic lap belt loading. The lap belt was placed on the mid-abdomen in horizontal position, just above the iliac crests, and was loaded by one or two pretensioners depending on the test. It should be noted that in these tests the velocity of lap belt reached much higher values (11–23 m/s) than the previous tests (2–5.6 m/s⁵ and 6 m/s⁶).

Foster et al.¹⁰ tested eight fixed-back PMHSs using a horizontal seat belt at the level of mid-umbilicus using single or dual pretensioner configurations. As in all previous tests, a symmetric loading (right and left) was implemented to reduce torsion and shear effects. The penetration was measured by a laser, which tracked the anterior aspect of abdomen. Peak anterior abdominal loads from 2.8 kN to 10.1 kN were recorded and peak penetration speeds varied from 4.0 m/s to 13.3 m/s. PMHS abdominal response corridors were developed and compared with previous data. Abdominal injuries were recorded in three tests (liver tears, 3 tests and spleen tears, 1 test).

Lamielle et al.¹¹ tested eight fixed-back PMHSs using symmetrical loading of a horizontally positioned lap belt. Two loading conditions were used: (1) a submarining condition (lower penetration rates 3.3–4.7 m/s and higher compression ratio—defined as the penetration divided by the initial thickness of abdomen ~40%) and (2) an out-of-position (OOP) condition (higher penetration rates 5–6 m/s and lower compression ratio ~30%). PMHSs sustained abdominal AIS score 2 to 3 injuries (e.g., 1 spleen contusion, 1 liver/pancreas contusions) in lower speed tests (submarining) and abdominal AIS 2 to 4 injuries (e.g., 2 deep lacerations of spleen, 1 pancreas laceration, 1 liver capsular tear) in the higher speed tests (OOP).

The main objective of this study is to investigate the biomechanical and injury responses of the human thorax and abdomen during the static deployment of two pretensioning systems. Compared with the previous PMHS studies, the subjects were positioned in production seats (not on rigid seats) and were restrained by a typical three-point belt system (not by a lap belt alone).

METHODS

Test Setup

Four PMHSs (Table 1) were positioned in production seats (front right passenger seat) in a standard passenger position (Table 2)¹² and were restrained using a standard (production) three-point belt system. Because it was hypothesized that human body characteristics, such as body mass index (BMI), will influence the biomechanical response and injury outcome in static pretensioning deployment tests, the PMHS was selected in a large BMI range from 15.6 to 31.2. The pretension forces in the belts were applied at two points (retractor and right anchorage), the dual pretensioner, or at all three locations, the triple pretensioner. All PMHSs procurement and experimentation procedures were approved by a University of Virginia Oversight Committee established by the Vice President for Research, which functions as an

TABLE 2. Schematic Representation of the Target Measurements for Subject and Seat Positioning

SB, seat back angle from horizontal (degrees)	60
HPT, H-point longitudinal distance from origin (mm)	420
HPTA, pelvic angle from horizontal (degrees)	22
H, head angle (degrees)	0
KL, lateral distance between the knees (mm)	230
TA, torso angle (angle of line from shoulder to H-point, from horizontal)	SB ± 5

The seat back inclination was not based on US NCAP guidelines and was representative of a reclined posture determined by authors. The H-point location on the subject was determined at the greater trochanter location. The seat height, position of the D-ring, and head restraint position were based on the US NCAP positioning guidelines.

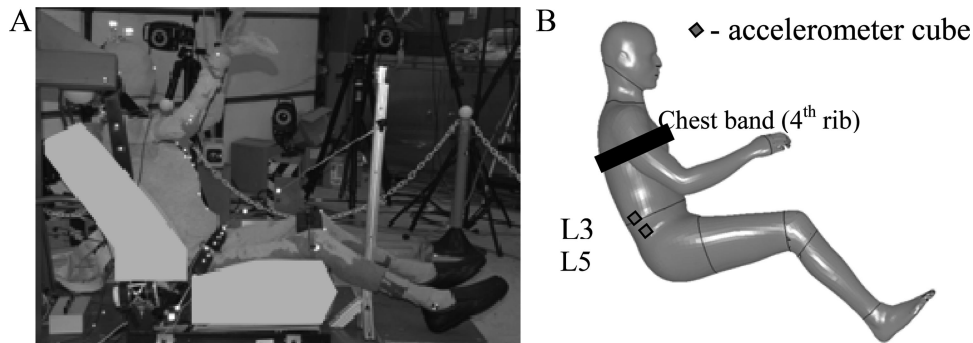


Figure 1. (A) Pretest configuration setup of PMHS (B) PMHS-accelerometer locations.

institutional review board for PMHS experimentation. PMHSs that were nonambulant for an extended period before death were excluded, as were subjects with bony pathology in the thorax as determined from pretest computed tomographic scans. The PMHSs that were selected for testing were preserved by freezing and confirmed free of the infectious diseases human immunodeficiency virus and hepatitis B and C. Immediately before testing, the subject's lungs were pressurized with 2.5 L of air. The tracheal tube through which the air was delivered was left open to the atmosphere after the single inflation cycle. In addition, to check the possibility of injury of PMHS urinary bladder under impact, an amount of water was added to it before testing. According to Hole,¹³ an adult urinary bladder may hold up to 600 mL of urine, and the desire to urinate usually starts when it contains about 150 mL. To simulate a critical condition, the bladder was filled with about 200 mL for each specimen before testing. A full body autopsy for each of the PMHS was performed by forensic pathologists after each test.

Instrumentation

The kinematic data of the belts and subjects, including anterior torso and abdomen deformation, were collected at 1,000 Hz using an optoelectronic stereophotogrammetric system consisting of 16 Vicon MX cameras that tracked the position of retro reflective spherical markers in a calibrated 3D space. The average error in the coordinate estimation of the system, evaluated previously, was under 1 mm.¹⁴ The calibration procedure, performed before the testing of each subject, established the position and orientation of the cameras with respect to one another. This information was used to reconstruct the 3D marker locations from multiple 2D camera images via a triangulation algorithm. Because the posterior region of subjects was covered by the seat structure, a set of accelerometer cubes (3 uniaxial accelerometers; Modesto 7264; Endevco, San Juan Capistrano, CA) were attached to the L3 and L5 vertebrae. The accelerometers allowed measuring the time histories of the spinal trajectories (at 10 kHz) (Fig. 1).

A portable static X-ray unit (Dynamic Imaging Systems, Inc., Rapid City, SD) was used to find the initial position and orientation of accelerometer cubes and to quantify the steady-state compression of the abdomen by measuring the pretest and posttest abdominal depths. A single

59-gauge chestband (Robert A. Denton, Rochester Hills, MI) was used at the fourth rib level to measure chest deformation and cross-sectional thoracic shape contour throughout the PMHS tests. The time histories of the belt forces were recorded using tension gauges (Model 3419; Lebow, Sensotec) on the shoulder belt between the D-ring and the right shoulder and on the lap belt at the buckle and anchorage attachments.

Data Analysis

For each subject, the kinematics of the markers (attached to the belts and thorax) was determined using a video-based optoelectronic stereophotogrammetric system methodology. An analysis of X-ray pretest pictures was performed to identify the pretest locations and orientations (in sagittal plane) of L3 and L5 accelerometers (Fig. 2). The dimensional scales (mm/pixel) of X-ray images were calibrated based on images of a metallic ball with known diameter (12.55 mm) inserted under the lap belt before testing (Fig. 2). The *x* and *z* coordinates of accelerometers were calculated based on the coordinates of the metallic ball recorded by the Vicon system before testing and the ball-accelerometer distances calculated from image analysis. The accelerometers were assumed to be in the same sagittal plane as the metallic ball, thus, to have the same *y* coordinate.

To study the whole kinematics of the PMHS and belts, LS-Dyna (LSTC, Livermore, CA) input files were developed using a customized Matlab (MathWorks, Inc, Natick, MA) program. In the LS-Dyna files, retroreflective markers and accelerometers were defined as nodes with prescribed displacement (Vicon markers) or acceleration (accelerometers) based on

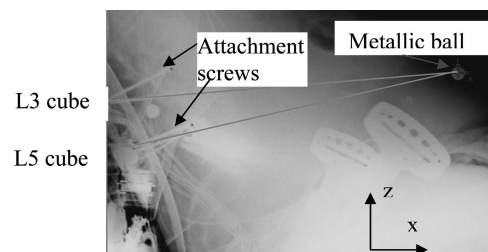


Figure 2. X-ray images of the PMHS (477) in the seat (pretest configuration).

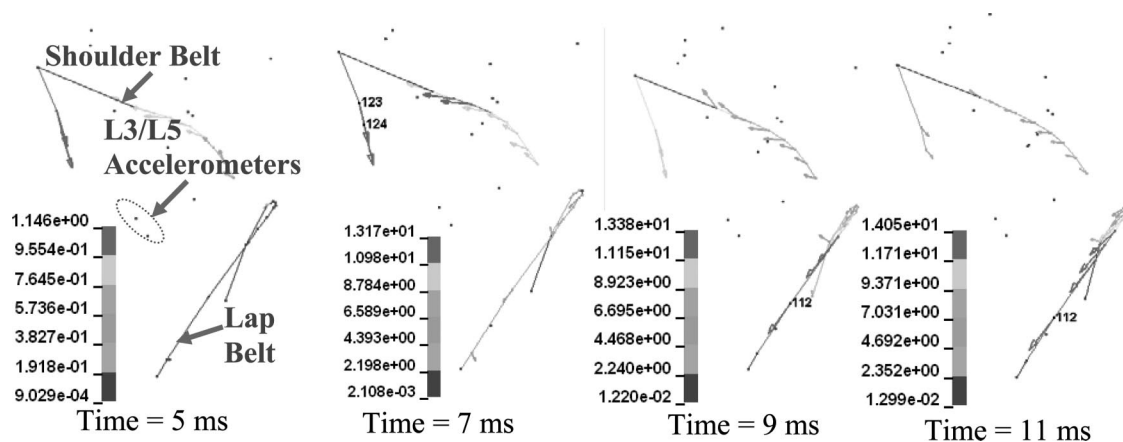


Figure 3. The resultant velocity of Vicor markers (attached to belts) and accelerometers (L3 and L5)—test 2.

corresponding test data recorded by Vicor systems or accelerometers (filtered with CFC 1000). These input files were run using a LS-Dyna processor and then, the results were visualized using a postprocessor (e.g., LS-Prepost). An example (test 2) with the positions of the nodes corresponding to the shoulder belt, lap belt, and the accelerometers together with their absolute velocity during pretensioning phase is illustrated in Figure 3. In addition to the velocity of each node, various kinematic measures (absolute or relative), including time history of penetration and penetration rate, were obtained directly from the finite element simulations of the tests.

Injury Risk Analysis

The PMHS data obtained in this study was combined with similar previously published data^{7–11} to perform an injury risk analysis (Table 3). Sample size and demographic statistics are demonstrated in Table 4, while detailed measurement information for each subject is summarized in Table 3. The combined dataset included the outcomes (the abdominal AIS values) and seven potential predictor variables (Table 3). The predictor variables included the following: peak lap belt force (PBF), abdominal displacement from belt loading (Disp), abdominal compression (Comp = belt displacement divided by subject's abdominal depth), velocity of belt into abdomen (Vel), the Abdominal Injury Criterion— $V_{\max}C_{\max}$ (the product of the maximum velocity, and the maximum compression),¹⁵ the Viscous Criterion— $V \times C$ (the maximum of the continuously calculated product of compression and velocity),¹⁶ and $F_{\max}C_{\max}$ (the product of the peak force and the maximum compression).¹⁷

Statistical analyses, which followed the injury risk analysis procedure presented in Ref. 18 were performed on the combined dataset using SAS software version 9.2 (SAS Institute, Cary, NC). Univariate logistic regression using both AIS score 2+ and AIS score 3+ as the binary outcomes and Pearson correlation analysis were conducted first to choose significant and linearly independent predictors. Univariate logistic regression was used to examine the effect of the seven predictor variables on the outcomes (AIS values), whereas the Pearson correlation analysis was used to determine correlated predictor variables. The results from the univariate logistic regression also

included the p values of two goodness-of-fit indices: deviance and Pearson's χ^2 , which test the null hypothesis that the model fits the data well. Furthermore, to evaluate the potential confounding effect, multivariate logistic regressions were conducted with the best potential predictor variables selected from the univariate logistic regression analyses. In addition, injury risk curves of the probability of injury as a function of predictor variables from logistic regression analyses were developed.

Survival analysis was also conducted to derive AIS score 2+ and AIS score 3+ injury risk curves and to approximate related injury thresholds for the best potential predictor variables selected from the logistic regression analyses. Interval censoring was applied to the data. For a no-injury case, it is assumed to be right censored to the extent of the highest stimulus no-injury case. For an injury case, it is assumed to be left-censored to the extent of the lowest stimulus injury case. The Akaike Information Criterion (AIC) and Bayesian Information Criterion (BIC) were used to compare the relative goodness-of-fit for different models under various distribution assumptions. Lower values of AIC and BIC indicate better fits of the model. Injury risk curves developed from survival analysis were compared with the curves developed from logistic regression.¹⁸

RESULTS

Test Data

The time histories of the belt forces recorded during the tests and filtered with SAE 1000 are presented in Figure 4. First, a force rise was observed in the shoulder belt followed after 1 ms by a force rise in the lap belts. The maximum force in the shoulder belt was about 2 kN to 2.2 kN in tests 1 and 2 and only 1.5 kN in the tests 3 and 4. Although the maximum force in lap belt was reached in about 3.5 ms in test 1 (triple pretensioning), ~5.5 ms was required in the other tests (double pretensioning). The maximum lap belt force (calculated as the average of anchorage and buckle forces) reached the highest value in test 1 (3.2 kN) and the lowest in test 4 (2.5 kN).

The time histories of abdominal compression ratio showed two different patterns (Fig. 5). The compression ratio

TABLE 3. Data Used in Development of Injury Risk Curves for Abdominal Loading by Belt Systems

Source	Number	Age, yr (Gender)	MAIS	Abdominal Depth (mm)	PBF (kN)	Belt Disp (mm)	Belt Comp (%)	Belt Vel (m/s)	$V_{\max}C_{\max}$	$V \times C$	$F_{\max}C_{\max}$
Trosseille et al. ⁹	PRT034	76(M)	2	230	6.11	68	29.6	8.2	2.42	1.13	1.8
Trosseille et al. ⁹	PRT035	81(M)	2	272	7.04	68	25.0	11.3	2.83	1.69	1.76
Trosseille et al. ⁹	PRT036	85(M)	4	235	10.3	76	32.3	11.5	3.72	2.1	3.33
Trosseille et al. ⁹	PRT038	64(F)	0	206	7.47	58	28.2	11.4	3.21	1.15	2.1
Trosseille et al. ⁹	PRT039	86(F)	2	207	7.59	62	30.0	11.7	3.5	0.85	2.27
Foster et al. ¹⁰	A1	24(M)	2	302	9.48	132.2	43.8	9.42	4.12	1.8	4.15
Foster et al. ¹⁰	A2	58(M)	0	356	10	126.1	35.4	6.89	2.44	1.11	3.55
Foster et al. ¹⁰	A3	80(M)	3	252	7.94	138.4	54.9	13.3	7.3	4.13	4.36
Foster et al. ¹⁰	A4	83(M)	3	259	9.64	130.3	50.3	8.51	4.28	2.03	4.85
Foster et al. ¹⁰	B1	85(M)	0	360	5.72	98.7	27.4	6.31	1.73	0.58	1.57
Foster et al. ¹⁰	B2	45(M)	0	258	4.98	92.3	35.8	6.13	2.19	1.1	1.78
Foster et al. ¹⁰	B3	59(M)	0	261	5.77	99.5	38.1	7.54	2.87	1.17	2.2
Foster et al. ¹⁰	C1	86(F)	0	191	3.1	49.4	25.9	5.35	1.38	0.57	0.8
Foster et al. ¹⁰	C2	86(F)	0	227	2.78	55.7	24.5	3.95	0.97	0.44	0.68
Hardy et al. ⁷	CB1	77(F)	0	239	4	79	33.1	3.2	1.06	0.7	1.32
Hardy et al. ⁷	CB2	77(F)	0	310	6.1	90	29.0	3.4	0.99	1.1	1.77
Hardy et al. ⁷	CB3	78(M)	0	208	3.1	75	36.1	2.1	0.76	0.8	1.12
Hardy et al. ⁷	CB4	78(M)	0	215	4.1	56	26.0	2.9	0.75	0.6	1.07
Hardy et al. ⁷	CB5	88(M)	0	288	4.3	95	33.0	3.7	1.22	0.9	1.42
Hardy et al. ⁷	CB6	88(M)	0	308	4.5	114	37.0	5.6	2.07	1.2	1.67
Steffan et al. ⁸	5	47(M)	0	229	.	76.9	33.6	n/a	n/a	n/a	n/a
Steffan et al. ⁸	6	49(M)	0	270	6	95.8	35.5	n/a	n/a	n/a	2.13
Steffan et al. ⁸	7	73(F)	0	262	4.9	109.4	41.8	n/a	n/a	n/a	2.05
Steffan et al. ⁸	8*	42.5(F)	0	239	7.4	75	31.4	n/a	n/a	n/a	2.32
Steffan et al. ⁸	9	58(M)	0	349	5.5	165.6	47.4	n/a	n/a	n/a	2.61
Steffan et al. ⁸	11	59(M)	0	294	10.6	103.7	35.3	n/a	n/a	n/a	3.74
Steffan et al. ⁸	12	50(M)	0	286	11.3	113.6	39.7	n/a	n/a	n/a	4.49
Steffan et al. ⁸	13	87(F)	0	266	.	150.2	56.5	n/a	n/a	n/a	n/a
Steffan et al. ⁸	14	66(M)	3	225	12.6	122.7	54.5	n/a	n/a	n/a	6.88
Steffan et al. ⁸	15	54(M)	0	277	10.9	157.3	56.8	n/a	n/a	n/a	6.2
Steffan et al. ⁸	16	95(F)	3	187	.	107.4	57.4	n/a	n/a	n/a	n/a
Steffan et al. ⁸	17	69(M)	3	278	9.2	153.4	55.2	n/a	n/a	n/a	5.08
Steffan et al. ⁸	18	84(F)	0	210	12.4	127	60.5	n/a	n/a	n/a	7.5
Current study	1	71(F)	2	367 [†]	6.49	89.7	24.44	5.08	1.24	0.374	0.79
Current study	2	70(M)	2	328 [†]	5.12	91.3	27.84	6.57	1.83	0.557	0.74
Current study	3	64(M)	0	226 [†]	4.75	47.3	20.95	4.47	0.94	0.478	0.54
Current study	4	70(M)	0	226 [†]	4.62	53.6	23.75	4.4	1.05	0.667	0.59

* The age of the subject in Steffan et al.'s test number 8 was cited as between 40 years and 45 years.

[†] Initial distance L5-mid-abdomen in normal seated posture.**TABLE 4.** Sample Size and Other Statistics for Combined PMHS Data

Sample Size	Age (yr)	PMHS With AIS 2 + Abdominal Injury	PMHS With AIS 3 + Abdominal Injury
37	Mean = 70	12	6
25 Men	Median = 73		
12 Women	Minimum = 24		
	Maximum = 95		

reached its maximum at about 80 ms to 90 ms in tests 1 and 2 (PMHS with higher BMI), but only in about 30 ms to 40 ms in tests 3 and 4. The time histories of abdominal penetration rates also exhibited different behaviors. In the tests 1 and 2, the abdominal penetration rate showed peaks at 4.6 m/s and 6.4 m/s, respectively, then a sudden decrease to almost zero level followed by a rise to a lower second peak. In the tests 3 and 4, the first peaks of penetration rates were recorded around 4.4 ms and were followed by a uniform decrease to zero level in about 20 ms.

To better understand different patterns of abdominal penetrations observed in the PMHS with higher BMI (tests 1 and 2) compared with the PMHSs with lower BMI (tests 3 and 4), the

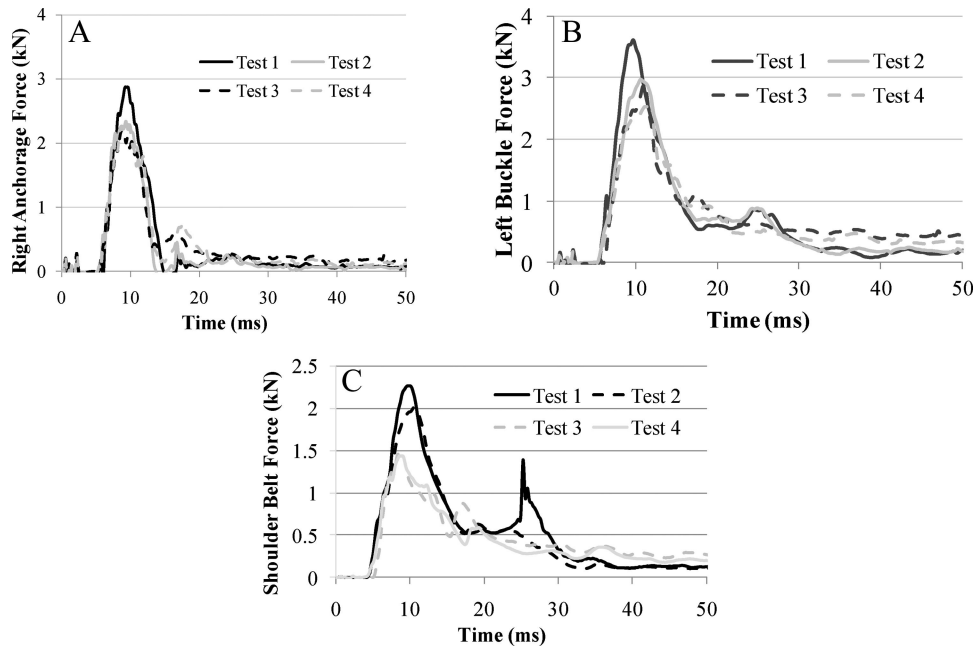


Figure 4. The time histories of lap belt forces at (A) right anchorage, (B) left buckle, and (C) shoulder belt.

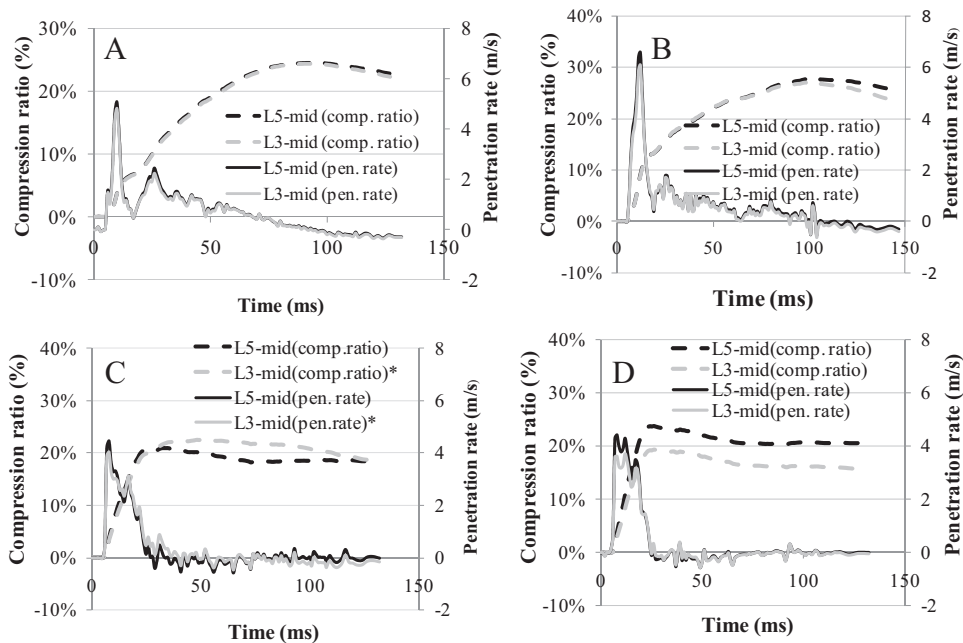


Figure 5. The penetration rates and compression ratios (A) test 1, (B) test 2, (C) test 3, and (D) test 4.

time histories of resultant displacement of lumbar accelerometers and lap belt markers were compared (Fig. 6). Although time histories of resultant displacement at lumbar locations showed similar trends in all tests with maximum displacements between 20 mm and 27 mm, different displacement patterns were observed for the lap belt markers. The markers on the lap belt showed almost ramp and

hold time histories in the case of the PMHS with lower BMI (tests 3 and 4). However, in the case of the PMHS with higher BMI (tests 1 and 2), the markers of the lap belt showed a sudden increase up to about 12 ms followed by a smoother increase up to about 90 ms to 100 ms.

One type of injury (laceration/tear of spleen capsule) was observed (Table 5) during the PMHS autopsies in PMHS

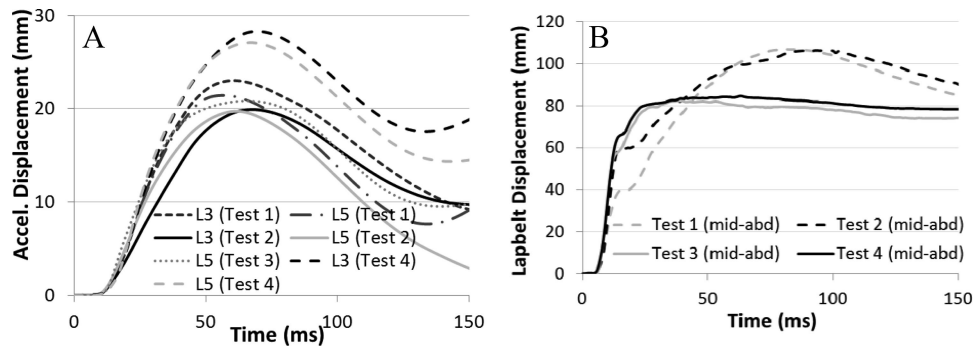


Figure 6. (A) The time history of accelerometer displacements (B) time histories of lap belt (markers) displacements.

TABLE 5. PMHS Autopsy Results

Test No. (PMHS No.)/ BMI	Injuries Recorded	AIS Score
1 (477)/31.2	1.3 cm spleen laceration/capsular tear	2
2 (478)/24.3	2 cm × 1.5 cm/spleen laceration/capsular tear	2
3 (459)/15.6	No injury	0
4 (458)/20.9	No Injury	0

TABLE 6. Peak Deflection From Chestband

Test	Deflection (mm)	Normalized Deflection
1	9.6	0.041
2	23.8	0.086
3	6.7	0.033
4	19.0	0.081

477 (test 1) and 478 (test 2). No injuries were observed in PMHS 459 (test 3) and 458 (test 4).

The chestband encircled the chest at the level of the fourth lateral rib for each PMHS. Table 6 provides peak

deflection values measured by the chestband during the PMHS tests. Peak deflections ranged from 9.6 mm to 23.8 mm. In Addition, these values were normalized using the PMHS chest depth. Peak normalized deflections ranged from 4.1% to 8.6%. This modest level of chest deflection (<10% chest deflection) is not expected to produce serious rib injury, but it is sufficient to produce the onset of injury (rib fractures). However, no rib fractures occurred during the tests.

Injury Risk Analysis

Results from the correlation analysis are shown in Table 7 for peak belt force, abdominal displacement, abdominal compression, velocity of belt into abdomen, the Abdominal Injury Criterion, the maximum Viscous Criterion, and $F_{\max}C_{\max}$. In Table 7, for each predictor variable, the top row presents the correlation coefficients and the bottom row presents the p value. The results show that many of the potential predictor variables were highly correlated, and therefore, coupling them in multivariate models would be inappropriate.

Table 8 shows the results of the univariate logistic regression analysis for the seven possible predictor variables and AIS score 2+ injuries. The velocity (model 4) had the

TABLE 7. Correlation Analysis of Potential Predictor Variables

	Depth	PBF	Disp	Comp (%)	Vel	$V_{\max}C_{\max}$	$V \times C$
PBF	0.093						
	0.601						
Disp	0.467	0.554					
	0.004	0.001					
Comp (%)	-0.048	0.632	0.847				
	0.776	<0.0001	<0.0001				
Vel	-0.066	0.737	0.271	0.396			
	0.758	<0.0001	0.200	0.055			
$V_{\max}C_{\max}$	-0.017	0.711	0.582	0.758	0.876		
	0.935	<0.0001	0.003	<0.0001	<0.0001		
$V \times C$	-0.034	0.590	0.595	0.790	0.697	0.910	
	0.875	0.002	0.002	<0.0001	0.000	<0.0001	
$F_{\max}C_{\max}$	0.007	0.909	0.720	0.874	0.663	0.850	0.786
	0.970	<0.0001	<0.0001	<0.0001	0.000	<0.0001	<0.0001

Bolded numbers appear in cells in which the correlation coefficient is greater than 70%, and the p values are less than 0.05.

TABLE 8. Univariate Logistic Regression Results for AIS 2+

Model Number	Predictor	Sample Size (No. Injured)	Constant <i>p</i>	Predictor <i>p</i>	Deviance <i>p</i>	Pearson's χ^2 <i>p</i>
1	PBF	34 (11)	0.017	0.053	0.162	0.426
2	Disp	37 (12)	0.176	0.444	0.065	0.293
3	Comp (%)	37 (12)	0.090	0.240	0.116	0.364
4	Vel	24 (9)	0.007	0.010	0.614	0.460
5	$V_{\max}C_{\max}$	24 (9)	0.009	0.014	0.565	0.536
6	$V \times C$	24 (9)	0.020	0.044	0.266	0.219
7	$F_{\max}C_{\max}$	34 (11)	0.021	0.120	0.151	0.394

Bolded row represents the best injury predictor for AIS 2+.

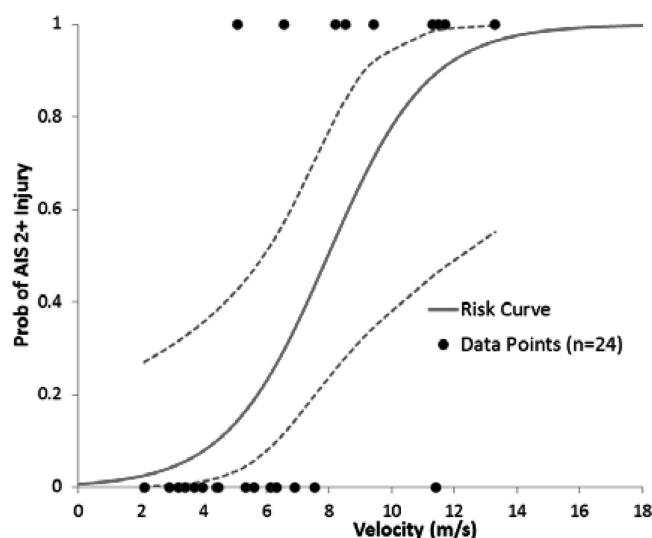


Figure 7. AIS score 2+ injury risk curve for velocity predictor from univariate logistic regression analysis.

best overall performance in terms of the deviance (0.614), the Pearson's χ^2 (0.460), and the significance of the predictor coefficient (0.010).

The corresponding risk equation for AIS score 2+ level injuries is as follows:

$$P_{AIS2+} = \frac{1}{1 + \exp^{-(-4.916 + 0.618Vel)}} \quad (1)$$

The risk curve of this equation, along with its 95% confidence interval (CI), is shown in Figure 7.

The same analysis was repeated for AIS score 3+ injuries. However, as shown in Table 4, the injury counts were reduced by considering this higher injury level. This posed a difficulty in achieving statistically significant predictors in the statistical models as illustrated in Table 9. The $F_{\max}C_{\max}$ (model 7) had the best overall performance for AIS score 3+ injury analysis. The corresponding risk equation for AIS score 3+ in terms of $F_{\max}C_{\max}$ is as follows:

$$P_{AIS3+} = \frac{1}{1 + \exp^{-(-4.359 + 0.753F_{\max}C_{\max})}} \quad (2)$$

The risk curve of this equation for AIS score 3+ injuries, along with its 95% CI, is shown in Figure 8.

The results from the multivariate logistic regression are given in Tables 10 and 11. Each of the aforementioned univariate models was made into a two-term multivariate model by linearly combining each of the potential predictor variables with the subjects' age and gender separately. The age and gender factors were insignificant for all the two-term models for both AIS score 2+ and AIS score 3+ injury analyses (Tables 10 and 11).

The survival analysis with interval censoring was further conducted to approximate risk curves and thresholds for AIS score 2+ and AIS score 3+ injury with the best predictor variables, Vel and $F_{\max}C_{\max}$, respectively. Various candidate distributions and goodness-of-fit statis-

TABLE 9. Univariate Logistic Regression Results for AIS 3+

Model Number	Predictor	Sample Size (No. Injured)	Constant <i>p</i>	Predictor <i>p</i>	Deviance <i>p</i>	Pearson's χ^2 <i>p</i>
1	PBF	34 (5)	0.007	0.025	0.903	0.911
2	Disp	37 (6)	0.011	0.064	0.675	0.450
3	Comp (%)	37 (6)	0.003	0.008	0.946	0.545
4	Vel	24 (3)	0.034	0.059	0.969	0.922
5	$V_{\max}C_{\max}$	24 (3)	0.134	0.146	0.999	0.999
6	$V \times C$	24 (3)	*	*	*	*
7	$F_{\max}C_{\max}$	34 (5)	0.001	0.015	0.943	0.940

* Regression did not converge.

Bolded row represents the best injury predictor for AIS 3+.

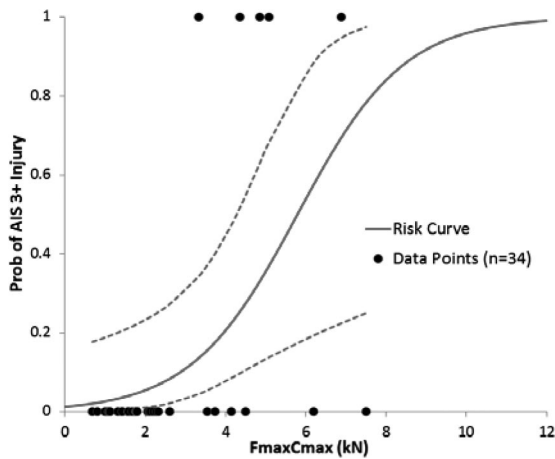


Figure 8. AIS score 3+ injury risk curve for $F_{\max}C_{\max}$ predictor from univariate logistic regression analysis.

TABLE 10. Multivariate Logistic Regression Results for AIS 2+

Model Number	Predictor	Age + Predictor		Gender + Predictor	
		Age (p)	Predictor (p)	Gender (p)	Predictor (p)
1	PBF	0.224	0.031	0.467	0.066
2	Disp	0.263	0.341	0.598	0.520
3	Comp (%)	0.335	0.247	0.502	0.238
4	Vel	0.801	0.011	0.669	0.010
5	$V_{\max}C_{\max}$	0.446	0.016	0.950	0.014
6	$V \times C$	0.811	0.049	0.652	0.044
7	$F_{\max}C_{\max}$	0.330	0.090	0.433	0.145

TABLE 11. Multivariate Logistic Regression Results for AIS 3+

Model Number	Predictor	Age + Predictor		Gender + Predictor	
		Age (p)	Predictor (p)	Gender (p)	Predictor (p)
1	PBF	0.093	0.018	0.946	0.037
2	Disp	0.066	0.036	0.570	0.082
3	Comp (%)	0.194	0.011	0.168	0.010
4	Vel	0.359	0.061	0.948	0.057
5	$V_{\max}C_{\max}$	*	*	0.959	0.134
6	$V \times C$	*	*	*	*
7	$F_{\max}C_{\max}$	0.135	0.014	0.940	0.024

* Regression did not converge.

tics, AIC and BIC, were assessed to determine the best fitted models for AIS score 2+ and AIS score 3+ injury (Tables 12 and 13). The lognormal distribution best represented the survival models with the predictor, Velocity, for AIS score 2+ injury, and with the predictor, $F_{\max}C_{\max}$, for AIS score 3+ injury.

The interval censoring survival curves for AIS score 2+ and AIS score 3+ injury are illustrated in Figures 9 and 10 correspondingly. The risk curves developed from the logistic regression analysis were added in Figures 9

TABLE 12. Goodness-of-Fit Statistics for VEL (AIS 2+) From Survival Analysis

Distribution	AIC	BIC
Exponential	63.681	64.859
Generalized Gamma	20.304	23.838
Logistic	27.927	30.283
Loglogistic	19.113	21.469
Normal	27.246	29.603
Lognormal	18.336	20.692
Weibull	19.690	22.046

Bolded row represents the best distribution for predictor Vel for AIS 2+.

TABLE 13. Goodness-of-Fit Statistics for $F_{\max}C_{\max}$ (AIS 3+) From Survival Analysis

Distribution	AIC	BIC
Exponential	70.352	71.878
Generalized Gamma	23.685	28.264
Logistic	30.035	33.087
Loglogistic	22.832	25.885
Normal	28.767	31.820
Lognormal	21.689	24.742
Weibull	22.492	25.545

Bolded row represents the best distribution for predictor $F_{\max}C_{\max}$ for AIS 3+.

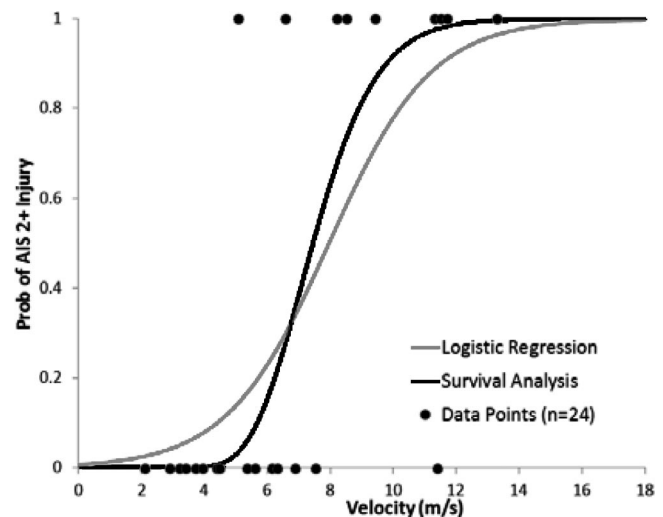


Figure 9. Comparison of AIS score 2+ risk curves for velocity as injury predictor.

and 10 for comparison purpose. For AIS score 2+ injury (Fig. 9), the corresponding risk equation for survival analysis is as follows:

$$P_{AIS2+} = \Phi\left(\frac{\log(Vel) - 2.008}{0.212}\right) \quad (3)$$

where Φ is the cumulative distribution function for the normal distribution.

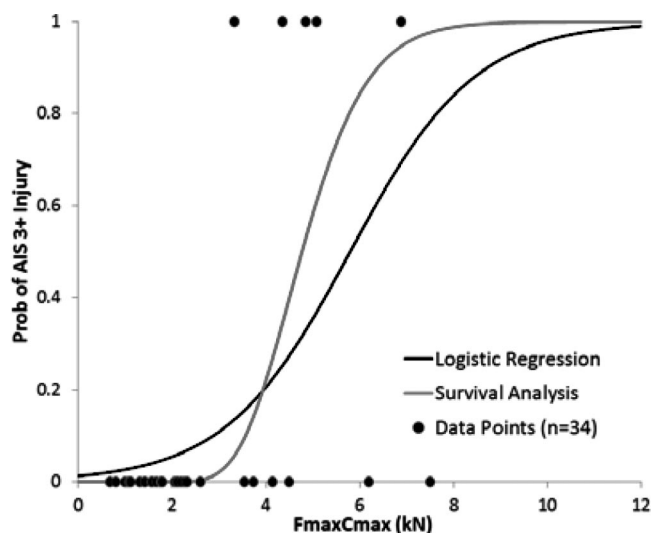


Figure 10. Comparison of AIS score 3+ risk curves for $F_{\max}-C_{\max}$ as injury predictor.

For AIS score 3+ injury (Fig. 10), the corresponding risk equation for survival analysis is:

$$P_{AIS3+} = \Phi\left(\frac{\log(F_{\max}C_{\max}) - 1.561}{0.228}\right) \quad (4)$$

DISCUSSION

Four PMHSs were tested to investigate the biomechanical and injury response of passenger during pretensioner loading. Although a PMHS model has anatomic similarities to a live person, its lack of muscle tone, circulation, and respiration may influence its overall biomechanical and injury response.¹⁹ A recent study performed on porcine specimens²⁰ showed that muscle tensing had a negligible effect at dynamic rates, hence the muscle tensing effect was assumed negligible in the pretensioner tests. Although air and fluid were pumped into PMHS lungs and urinary bladder just before impact, the effect of circulation in a living person is not known. The material properties and injury response of abdominal organs may also be different in PMHS than in live human because of the possible changes caused by tissue degradation after death or by the PMHS preservation process (e.g., freezing effect). Although several studies investigated the effect of freezing on the abdominal organs, the results reported showed different conclusions, possibly because of different testing conditions (e.g., tension, compression) or origin (e.g., porcine, bovine). For example, Tamura et al.²¹ showed that freezing has no significant effect on porcine liver specimens in compression, but Santiago et al.²² performed tensile tests on bovine specimens and showed that freezing reduces significantly the average failure strain but keeps almost the same the failure stress. Therefore, future studies should further investigate the effect of preservation on human abdominal tissues at loading types and rates corresponding to pretensioner loadings (finite element simulations with human models may be used to identify these loading conditions).

Even though the dynamic loading of the passenger during the crash was neglected here, as in all previous studies, the belt loading was simulated more accurately by the seat and three-point belt system used in this study. Of course, using a production seat required the measurement of the lumbar spine motion during testing rather than fixing the spine as in previous tests. Consequently, the calculation of abdominal penetration was significantly more challenging. Abdominal penetration was also more difficult to define because of the shape of lumbar spine during the impact. Although the motion of PMHS back was measured at two locations (L3 and L5), the location which provided the highest compression ratio (L5) was used for calculating the abdominal penetration.

Two different patterns of abdominal penetration rate were observed in the PMHS tests. Although in the PMHSs with lower BMI, the penetration rate simply increased to a peak then decreased to zero, two significant peaks separated by a sudden decrease to almost zero value were observed in the PMHSs with higher BMI. This variation of penetration rate could be explained by the higher abdominal mass that needed to be compressed in the obese PMHSs, which required a longer time interval until equilibrium was reached. This behavior may also been associated with the abdominal injuries recorded in the PMHS with higher BMI, but more tests should be performed to verify this hypothesis. The injury mechanism of spleen lacerations observed in the pretensioner tests is challenging to identify based only on the exterior deformation of abdomen. The spleen is held in position by various peritoneal folds, and as other several abdominal organs like the liver is protected by thoracic cage. Although no rib fractures were observed in the tests, the spleen injuries may be associated with a “crushing” of internal organs or with the pressure waves propagated through the abdomen during its compression. The role of higher abdominal inertia associated with the higher BMI subjects may also influence the loading and boundary conditions of the spleen during testing, especially because the spleen was close to, but not on the loading path of the lap belt. The results of previous studies on the effect of the abdominal fat on abdominal trauma recorded in traffic accidents are not consistent. Although the results of two studies^{23,24} based on the Crash Injury Research Engineering Network database indicate that the overweight subjects have a decreased incidence of abdominal injuries, the results of other recent statistical studies^{25,26} showed an opposite effect. Therefore, it is believed that using high-speed medical imaging in future abdominal tests or computer simulations may provide a better understanding of abdominal organ motion and spleen trauma during belt loading. Although the types of abdominal injuries obtained using a PMHS model may be not identical to those a human would experience because of factors such as lack of active musculature, tissue lividity, and autolysis, the spleen injuries observed in two tests are frequently observed in traffic accidents. The spleen was reported as the first and the second most commonly injured abdominal organ in the frontal crashes for passenger and for drivers, respectively.²⁷

The injury risk analysis showed Velocity and $F_{\max}C_{\max}$ to be the best predictors of AIS score 2+ and AIS score 3+ injury, respectively; however, the CIs for the logistic regression analysis are quite broad because of small sample size, so a bootstrap

approach may be used in the future to reduce the CI size.²⁸ This result was different from the findings in the experiments of Kent et al.²⁹ In that study, “peak belt tension and abdominal penetration” were the best predictors of injury outcome, regardless of the penetration rate. The possible reasons for the difference might be the coverage area of the lap belt and the subject positions during the testing. In Ref. 29, Kent et al. investigated the abdominal responses by using pediatric swine subjects to represent 6-year-old human child. The lap belt covered proportionally more abdominal area in porcine subjects than in adult PMHS subjects. Moreover, the porcine subjects were tested in the supine position, whereas the PMHS subjects used in this study were in the upright, seated position. Because the abdominal organs are quite mobile,³⁰ this could affect the injury outcome.

The goodness-of-fit statistics in the survival analysis suggested that the best distribution to represent the injury risk curves was the lognormal distribution. Indeed, some parametric models such as Weibull, log-logistic, and lognormal distributions with a lower bound at zero had been shown to better represent the injury risk data.^{31–33} Although Weibull distribution has been chosen as central to the parametric analysis of failure time data among all available parametric survival models, this study showed that the lognormal distribution could also be a good option for modeling risk curves for abdominal injuries.

When comparing the recent work by Rouhana et al.¹⁸ with a recent study which analyzed previous published abdomen test data (33 samples), some interesting findings were observed. First, the univariate logistic regression analysis for AIS score 2+ showed that velocity was the best predictor according to the deviance and Pearson's χ^2 , whereas $V_{\max}C_{\max}$ was found the best predictor for AIS score 2+ in Ref. 18. In Table 8, similar deviance and Pearson's χ^2 were obtained between velocity and $V_{\max}C_{\max}$, whereas velocity had slightly smaller p value of predictor. Because of the small sample size, the two predictors were competitive, and further analyses on comparing of the two variables could be conducted when large sample size is available. Similarly, in Table 9 for AIS score 3+ case, similar deviance and Pearson's χ^2 were obtained between $F_{\max}C_{\max}$ and $V_{\max}C_{\max}$, while $F_{\max}C_{\max}$ provided a much smaller predictor p value; therefore, $F_{\max}C_{\max}$ was elected as the best predictor but not $V_{\max}C_{\max}$, which was chosen as the best predictor for AIS score 3+ in Ref. 18. Second, the goodness-of-fit statistics in Tables 12 and 13 showed that the lognormal distribution best fitted for injury curves for both AIS score 2+ and AIS score 3+ in survival analysis. Although Rouhana et al.¹⁸ proposed the normal distribution to be the best distribution, the values of the Anderson-Daling and correlation coefficient criteria, used in their study tended to be very close (1.250–1.319 and 0.996–0.999, respectively). Therefore, these two criteria may not be good discriminators in the case of abdominal injury investigation. Third, our study concluded that most of the correlations between the predictors were insignificant and, specifically, that age and gender effects were insignificant. Rouhana et al. reached similar conclusions as well.¹⁸ Although most epidemiologic and statistical studies considered age and gender as influential factors on the responses of interest, this study showed that age and gender were not significant effects on

the injury outcome based on the multivariate logistic regression for both AIS score 2+ and AIS score 3+ cases. This suggests that the abdominal injury is independent of subjects' age and gender when combined with potential predictor variables in the multivariate analyses, and these two factors can be reasonably omitted in the injury risk analysis. This does not necessarily mean that age and gender are inapplicable predictor variables in general; rather it means that they were not significant in this sample set of outcomes fitted by two-term models. It should be also mentioned that the results of all statistical analyses may depend on age distribution of specimens, which in this study, as in the majority of data reported in trauma literature, are mostly in the range of old specimens.

A limitation in the injury risk analysis may come from different test setups used in different tests (Table 14). The current tests and the tests by Steffan et al.⁸ were performed with PMHS in a seated posture, but all other tests^{7,9,10} were performed in upright posture. A previous study³⁴ showed that the posture effect has lower influence than subject-to-subject variations. However, the influence of different positions of lap belt on the abdominal response and injury is unknown. Although the lap belt was positioned at the level of umbilicus in all tests, some differences were recorded in the belt path. Although the lap belt was almost horizontal in the tests run in the upright posture, a path closed to that experienced by a restrained automobile occupant was realized in the seated posture. In addition, in current tests and in two tests of Hardy et al.,⁷ the lap belt was positioned below the anterior-superior iliac spine of the pelvis (in position), in all other tests the lap belt was positioned above anterior-superior iliac spine to simulate a submarining loading condition (OOP). Therefore, future studies may investigate the influence of lap belt path on the abdominal injury response. In current tests, as in all previous tests, the inertia of the human body during deceleration phase were neglected. To better replicate the real world impacts, future studies may also consider testing the high pretensioners in sled test configurations with acceleration pulse corresponding to vehicle crashes. This recommendation is supported by the results of recent studies which showed that higher risk of abdominal injuries in obese occupants.^{25,26} In addition to statistical injury analysis obtained from test data, it is believed numerical simulations with accurate human model may provide insights in the injury mechanism and optimizing the pretensioner designs.

TABLE 14. Test Setup, Initial Positioning, and PMHS Conditions Used in Previous and Current Tests

Source	PMHS Position	Lap Belt Position Relative to ASIS	Shoulder Belt
Trosseille et al. ⁹	Upright/fixed back	Above	No
Foster et al. ¹⁰	Upright/fixed back	Above	No
Hardy et al. ⁷	Upright/free (5*)/fixed (1*)-back	Below (2*)/above (4*)	No
Steffan et al. ⁸	Rotated on a rigid seat (45°)	Above	No
Current study	Rotated on a production seat	Below	Yes

* Number of specimens tested.

CONCLUSIONS

The test data recorded in four PMHS static deployment pretensioner tests are reported in this study. Two different patterns were observed in the time histories of abdominal penetration rate and injury response in the PMHS with lower and higher BMI. Although the abdominal penetration rate showed sharp variations in the two PMHSs with higher abdominal mass, more uniform decrease was observed in other two subjects. Abdominal injuries (spleen lacerations) were observed in two PMHSs with higher BMI, but no trauma in other two PMHSs. An injury risk analysis performed using the test data obtained in this study and similar data from literature showed that the belt velocity and $F_{\max} C_{\max}$ are the best predictors for AIS score 2+ and for AIS score 3+ injuries, respectively. More tests in the same test setup are recommended for a more robust injury risk analysis and, hopefully, for better understanding the injury mechanism of abdominal injuries.

AUTHORSHIP

C.D.U., D.B., D.L., P.R. and M.S. designed and performed the experiments. D.L. and P.R. managed and analyzed Vicon data. D.B. managed and analyzed load data collection. Y.-C.L. performed the statistical analysis and interpreted the results. M.S. analyzed injury data. C.D.U. overviewed the entire project, analyzed the whole data set, and prepared the manuscript. All co-authors reviewed the manuscript and revision.

DISCLOSURE

The authors declare no conflicts of interest.

REFERENCES

1. Fifth/Sixth Report to Congress. *Effectiveness of Occupant Protection Systems and Their Use* (Report No. DOT-HS-809-442). U.S. Department of Transportation: Washington, DC; 2001.
2. Adam, T, Untaroiu, C.D. Identification of occupant posture using a bayesian classification methodology to reduce the risk of injury in a collision. *Transportation Research Part C: Emerging Technologies*, 2011, 19(6):1078–1094.
3. Bose D., Crandall J.R., Untaroiu C.D., Maslen E.H. Influence of pre-collision occupant state parameters on injury outcome in a frontal collision. *Accident Analysis and Prevention*, 2010, 42(4):1398–1407.
4. Zellmer H, Kahler C, Eickhoff B. Optimised pretensioning of the belt system: A rating criterion and the benefit in consumer tests. Proceeding of ESV Conference. Washington, D.C., USA 2005.
5. Douglas C, Fildes B, Gibson T, et al. *Factors Influencing Occupant to Seat Belt Interaction in Far Side Crashes*. 51th Proceedings of the Association for the Advancement of Automotive Medicine. Birmingham, Alabama, USA 2007;319–342.
6. Miller MA. The biomechanical response of the lower abdomen to belt restraint loading. *J Trauma*. 1989;29:1571–1584.
7. Hardy WN, Schneider LW, Rouhana SW. Abdominal impact response to rigid-bar, seatbelt, and airbag loading. *Stapp Car Crash J*. 2001;45:1–32.
8. Steffan H, Hofinger M, Parenteau C, et al. *Abdominal Responses to Dynamically Lap Belt Loading*. Proceeding of IRCOBI Conference. Munich, Germany 2002.
9. Trosseille X, Le-Coz JY, Portier P, Lassau JP. Abdominal response to high-speed seatbelt loading. *Stapp Car Crash J*. 2002;46:71–79.
10. Foster CD, Hardy W, Yang KH, King AI, Hashimoto S. High-speed seatbelt pretensioner loading of the abdomen. *Stapp Car Crash J*. 2006;50:27–51.
11. Lamielle S, Vezin P, Verriest JP, Petit P, Trosseille X, Vallancien G. 3D deformation and dynamics of the human cadaver abdomen under seatbelt loading. *Stapp Car Crash J*. 2008;52:267–294.
12. Robbins DH, Schneider LW, Snyder RG, et al. *Seated Posture of Vehicle Occupants*. Proceeding of the 27th Stapp Car Crash Conference. P-134. Warrendale: 1983;199–224.
13. Hole JW. *Human Anatomy and Physiology*. 2nd ed. William C. Brown. Dubuque, IA: 1981.
14. Lessley DJ, Purtseov SV, Shaw CG, Parent DP, et al. *Assessment and Validation of a Methodology for Measuring Anatomical Kinematics During Impact Loading*. Proceedings of the 37th International Workshop Injury Biomechanics Research. Scottsdale, Arizona, USA 2010.
15. Rouhana SW, Lau IV, Ridella SA. Influence of velocity and forced compression on the severity of abdominal injury in blunt, nonpenetrating lateral impact. *J Trauma*. 1985;25:490–500.
16. Viano DC, Lau IV. *Thoracic Impact: A Viscous Tolerance Criterion*. 10th International Conference on the Enhanced Safety of Vehicles, 104–114, SAE Technical Paper No. 1985:856025. Oxford, UK.
17. Rouhana SW. Abdominal injury prediction in lateral impact—an analysis of the biofidelity of the Euro-SID abdomen. *Stapp Car Crash J*. 1987;54:95–104.
18. Rouhana SW, El-Jawahri RE, Laituri TR. Biomechanical considerations for abdominal loading by seat belt pretensioners. *Stapp Car Crash J*. 2010; 381–406.
19. Crandall JR, Bose D, Forman J, et al. Human surrogates for injury biomechanics research. *Clin Anat*. 2011;24:362–371.
20. Kent R, Stacey S, Kindig M, et al. Biomechanical response of the pediatric abdomen, Part 1: development of an experimental model and quantification of structural response to dynamic belt loading. *Stapp Car Crash J*. 2006;50:1–26.
21. Tamura A, Omori K, Miki K, Lee JB, Yang KH, King AI. Mechanical characterization of porcine abdominal organs. *Stapp Car Crash J*. 2002;46:55–69.
22. Santago AC, Kemper AR, McNally C, Sparks JL, Duma SM. Freezing affects the mechanical properties of bovine liver. *Biomed Sci Instrum*. 2009;45:24–29.
23. Arbabi S, Wahl WL, Hemmilla MR, Kohoyda-Inglis C, Taheri PA, Wang SC. The cushion effect. *J Trauma*. 2003;54:1090–1093.
24. Wang SC, Bednarski B, Patel S, et al. *Increased Depth of Subcutaneous Fat Is Protective Against Abdominal Injuries in Motor Vehicle Collisions*. In 47th Proceedings of the Association for the Advancement of Automotive Medicine. Lisbon, Portugal 2003.
25. Ryb GE, Dischinger PC. Injury severity and outcome of overweight and obese patients after vehicular trauma: A crash injury research and engineering network (CIREN) study. *J Trauma*. 2008;64:406–411.
26. Zarzaur BL, Marshall SW. Motor vehicle crashes obesity and seat belt use: A deadly combination? *J Trauma*. 2008;64:412–419; discussion 419.
27. Elhagediab AM, Rouhana SW. *Patterns of Abdominal Injury in Frontal Automotive Crashes*. Proceedings of the 16th International Technical Conference on Experimental Safety Vehicles. Windsor, Ontario, Canada 1998;327–337.
28. Lu Y-C, Untaroiu CD. A bootstrap approach for lower injury levels of the risk curves. *Comput Meth Programs Biomed*. In press. <http://dx.doi.org/10.1016/j.cmpb.2011.03.015>
29. Kent R, Stacey S, Kindig M, et al. Biomechanical response of the pediatric abdomen, Part 2: Injuries and their correlation with engineering parameters. *Stapp Car Crash J*. 2008;52:135–166.
30. Rouhana SW. Biomechanics of abdominal trauma. In Nahum AM, Melvin JW, eds. *Accidental Injury: Biomechanics & Prevention*. 2nd ed. New York: Springer-Verlag; 2002;405–453.
31. Kent RW, Funk JR. *Data Censoring and Parametric Distribution Assignment in the Development of Injury Risk Functions From Biomechanical Data*. Paper 2004-01-0317. Society of Automotive Engineers 2004 World Congress & Exhibition. Detroit, Michigan, USA.
32. Kennedy EA, Hurst WJ, Stitzel JD, et al. Lateral and posterior dynamic bending of the mid-shaft femur: fracture risk curves for the adult population. *Stapp Car Crash J*. 2004;48:27–51.
33. Di Domenico L, Nusholtz G. *Comparison of Parametric and Non-parametric Methods for Determining Injury Risk*. Paper 2003-01-1362. Society of Automotive Engineers 2003 World Congress & Exhibition. Detroit, Michigan, USA
34. Beillas P, Lafon Y, Smith FW. The effects of posture and subject-to-subject variations on the position, shape and volume of abdominal and thoracic organs. *Stapp Car Crash J*. 2009;53:127–154.